Upscaling of dispersion in gas-liquid absorption on an inclined surface

Morteza Dejam [1,*] and Hassan Hassanzadeh [2,†]

[1]*Department of Energy and Petroleum Engineering, College of Engineering and Physical Sciences, University of Wyoming, 1000 E. University Avenue, Laramie, Wyoming 82071-2000, USA*

[2]*Department of Chemical and Petroleum Engineering, Schulich School of Engineering, University of Calgary, 2500 University Drive NW, Calgary, Alberta T2N 1N4, Canada*

(Received 4 June 2023; accepted 17 August 2023; published 13 September 2023)

We extend the Taylor-Aris dispersion theory to upscale the gas absorption into a viscous incompressible liquid flowing along an inclined surface. A reduced-order model of advection-dispersion-reaction is developed with the aid of Reynolds decomposition and cross-sectional averaging techniques. The upscaled model allowed evaluation of the dispersion, advection, and absorption kinetics as a function of the Peclet number (Pe) and the Damköhler number (Da). The transport and kinetics parameters for the limiting cases of nonabsorption and absorption dominant are also evaluated. The upscaled model is solved analytically, and the obtained solution is used to evaluate the upscaled mass transfer between the gas and liquid. The results for the overall Sherwood number identify three regions: (i) advection dominant, (ii) transition where both advection and absorption play a role, and (iii) absorption dominant. The scaling relation between the Sherwood number (Sh) and the Da for the last region was determined to follow $\mathrm{Sh} \sim \mathrm{Da}^{1/2}$. It is also revealed that in the first two regions, the Sherwood number versus the Peclet number exhibits a bell-shaped (or Gaussian) behavior, suggesting an optimal Pe that maximizes mass transfer between gas and liquid in these regions. The model and insights presented have the potential to be applied in a wide range of industrial separation processes involving the interaction of a gas exposed to a liquid flowing downward on an inclined surface under gravity.

DOI: 10.1103/PhysRevE.108.035104

I. INTRODUCTION

Gas absorption into a liquid phase is of fundamental significance for the separation process and is extensively implemented in numerous industrial applications such as carbon capture [1,2]. Generally, gas absorption is often utilized to separate undesirable components from a gas stream [3,4], gas dissolution and exsolution [5], or to produce a chemical [6]. Therefore, numerous theoretical and experimental studies have been conducted to enhance our understanding of the process, and these studies continue to evolve [7]. In this process, a gas is often exposed to a laminar, viscous incompressible liquid flowing downward on an inclined surface under gravity. The gas solute is absorbed and eliminated by the underlying liquid flow, while the mass transfer of the solute takes place from the gas phase to the liquid phase across the interface of these two phases. The contact time between the gas solute and liquid is long enough to establish a steady velocity profile [8]. Such dynamics are frequently needed for gas absorption and other important applications, including falling film microreactors, heat exchangers, and desalination processes [9–14].

The gas-liquid mass transfer has been studied in wetted wall columns [15], on inclined surfaces [16], and on spheres [17], where the liquid and gas phases can be water and carbon dioxide-containing gas streams, and amine solutions and carbon dioxide-containing gas streams, among others. While the dispersion of a gaseous solute during gas absorption through the gas-liquid interface [18–20] is key for the evaluation of the performance of the separation process, less attention has been paid to this subject until now.

Taylor [21] and Aris [22] established the mathematical foundation of shear-induced solute dispersion, or the so-called Taylor-Aris theory. Many significant extensions have been made to the Taylor-Aris theory to determine the solute dispersion for different fluids (Newtonian, non-Newtonian, and viscoelastic) [23–25], flows (pressure-driven or Poiseuille, electro-osmotic, and cross-flow) [26–28], geometries (circular, rectangular, triangular, and elliptical conduits) [29–31], wall conditions (adsorbing, constant concentration, porous, permeable, and rough) [32–36], phases (one phase, two phase, and multiphase) [37,38], and porous media (matrix-fracture and stratified media) [39,40].

However, the derivation of the dispersion for gas solute absorption into a liquid phase with advection, diffusion, and reaction on an inclined surface, despite its significance in numerous chemical engineering applications, has not been reported.

In this work, the Taylor-Aris dispersion theory is extended to study the gas solute transport in a liquid phase on an inclined surface due to the gas absorption at the interface between the gas and liquid phases. First, the Stokes equation describing the fully developed laminar flow subject to a no-shear stress condition at the liquid-gas interface and a no-slip condition at the surface is applied to derive the velocity profile of the liquid. Then, the gas solute transport in the liquid phase

*Corresponding author: mdejam@uwyo.edu
†Corresponding author: hhassanz@ucalgary.ca

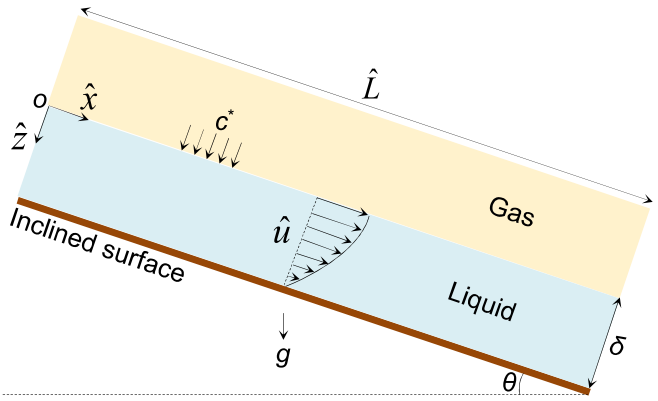

FIG. 1. Schematic diagram of gas absorption into a liquid phase with advection, diffusion, and reaction on an inclined surface.

is modeled by implementing the unsteady two-dimensional advection-diffusion-reaction equation in conjunction with a constant gas concentration at the gas-liquid interface and a zero-gas flux at the wall surface. Finally, the extended reduced-order model of advection-dispersion-reaction solute transport due to a laminar flow of a viscous incompressible liquid with gas absorption on an inclined surface is established using Reynolds decomposition and cross-sectional averaging. The resulting model provides an evaluation of advection, dispersion, and absorption kinetics coefficients, which are then utilized to analyze the process. In addition, the average gas solute concentration in the liquid phase and the Sherwood number (Sh) are derived and studied.

The rest of this work is structured as follows. First, the physical system and underlying assumptions are presented. Subsequently, the reduced-order model is established. Then, the obtained results are discussed, followed by a summary of the findings and concluding remarks.

II. PHYSICAL SYSTEM AND ASSUMPTIONS

The schematic diagram of the physical system under consideration in this study is shown in Fig. 1. The system involves gas absorption into a downward-flowing laminar, viscous incompressible liquid on an inclined surface, where the effects of gravity, advection, diffusion, and reaction are considered. The inclined surface makes an angle θ with the horizontal plane. The liquid phase inlet serves as the reference point for the direction along the surface ($\hat{x}$), while the gas-liquid interface serves as the reference point for the direction perpendicular to the surface ($\hat{z}$). The length and the thickness of the liquid are $\hat{L}$ and δ, respectively. The liquid flow is fully developed, and the velocity profile is $\hat{u}$. The gas solute equilibrium solubility in the liquid is c^*, and the solute-free liquid phase enters the domain at $\hat{x} = 0$. The physical properties of the liquid, such as viscosity, μ, and density, ρ, are taken as constant. Gravitational acceleration is g and it acts in a vertical downward direction.

III. MATHEMATICAL MODELING

The Stokes equation, as a second-order linear ordinary differential equation, is applied to describe the fully developed laminar flow of a liquid phase on an inclined surface:

$$\mu \frac{d^2\hat{u}}{d\hat{z}^2} + \rho g \sin\theta = 0. \tag{1}$$

Equation (1) can be solved subject to a no-shear stress condition at the liquid-gas interface ($\hat{z} = 0$) and a no-slip condition at the surface ($\hat{z} = \delta$):

$$\frac{d\hat{u}(\hat{z} = 0)}{d\hat{z}} = 0 \tag{2}$$

$$\hat{u}(\hat{z} = \delta) = 0, \tag{3}$$

which results in the following analytical solution for the velocity profile of the liquid:

$$\hat{u}(\hat{z}) = \frac{\rho g \delta^2 \sin\theta}{2\mu}\left[1 - \left(\frac{\hat{z}}{\delta}\right)^2\right]. \tag{4}$$

The cross-sectional average velocity of the liquid, $\bar{\hat{u}}$, is defined as follows:

$$\bar{\hat{u}} = \frac{\int_0^\delta \hat{u}(\hat{z})d\hat{z}}{\int_0^\delta d\hat{z}} = \frac{\rho g \delta^2 \sin\theta}{3\mu}. \tag{5}$$

If $\hat{u}$ is scaled by $\bar{\hat{u}}$, the nondimensional velocity profile of the liquid, u, will be obtained as

$$u(z) = \frac{\hat{u}(\hat{z})}{\bar{\hat{u}}} = \frac{3}{2}(1 - z^2), \tag{6}$$

where $z = \hat{z}/\delta$ is the nondimensional direction perpendicular to the surface [41].

The mass balance leads to the following unsteady two-dimensional advection-diffusion-reaction equation for the nondimensional concentration of gas solute in the liquid phase, $c(x, z, t)$:

$$\frac{\partial c}{\partial t} + \mathrm{Pe}\, u(z)\frac{\partial c}{\partial x} + \mathrm{Da}\, c = \frac{\partial^2 c}{\partial x^2} + \frac{\partial^2 c}{\partial z^2}, \tag{7}$$

where $c = \hat{c}/c^*$, $t = D\hat{t}/\delta^2$, $x = \hat{x}/\delta$, the Peclet number (Pe) $= \bar{\hat{u}}\delta/D$, and the Damköhler number (Da) $= \kappa\delta^2/D$, in which $\hat{c}$ is the dissolved gas concentration in the liquid phase, $\hat{t}$ is the time, t is the nondimensional time, D is the gas diffusivity in the liquid phase, x is the nondimensional direction along the surface, Pe is defined as the advection-to-diffusion transport, κ is the first-order reaction rate constant, and Da is defined as the reaction-to-diffusion transport.

Equation (7) can be solved using the following initial and boundary conditions:

The initial gas concentration in the liquid phase is zero:

$$c(x, z, t = 0) = 0. \tag{8}$$

At the inlet, the liquid phase begins as a pure liquid, implying that the gas concentration is zero:

$$c(x = 0, z, t) = 0. \tag{9}$$

The solute gas concentration gradient (or flux) is zero at the outlet of the liquid phase when the liquid thickness is much smaller than the liquid length, $\delta \ll \hat{L}$,

$$\frac{\partial c(x = L, z, t)}{\partial x} = 0, \tag{10}$$

where $L = \hat{L}/\delta$ is the nondimensional length of the liquid.

At the gas-liquid interface, the gas concentration is constant and equal to the equilibrium solubility of the gas in the liquid phase:

$$c(x, z = 0, t) = 1. \tag{11}$$

The solute gas concentration gradient (or flux) is zero at the inclined wall surface:

$$\frac{\partial c(x, z = 1, t)}{\partial z} = 0. \tag{12}$$

Using Reynolds decomposition as an approach to separate the cross-sectional average and fluctuation components of a variable [41] results in the following expressions for c and u, respectively:

$$c(x, z, t) = \bar{c}(x, t) + c'(x, z, t) \tag{13}$$

and

$$u(z) = \bar{u} + u'(z) = 1 + u'(z), \tag{14}$$

where $\bar{c}$ and $\bar{u}$ are the nondimensional cross-sectional average gas concentration and velocity components, and c' and u' are the nondimensional gas concentration and velocity fluctuation components, which satisfy the following equations:

$$\bar{c}(x, t) = \int_0^1 c(x, z, t)dz, \tag{15}$$

$$\bar{u} = \int_0^1 u(z)dz = 1, \tag{16}$$

$$\int_0^1 c'(x, z, t)dz = 0, \tag{17}$$

and

$$\int_0^1 u'(z)dz = 0. \tag{18}$$

Equations (17) and (18) indicate that the cross-sectional averages of c' and u' are zero.

Replacing for c in Eqs. (7)–(12) from Eq. (13) leads to

$$\frac{\partial \bar{c}}{\partial t} + \frac{\partial c'}{\partial t} + \mathrm{Pe}\, u(z)\frac{\partial \bar{c}}{\partial x} + \mathrm{Pe}\, u(z)\frac{\partial c'}{\partial x} + \mathrm{Da}\, \bar{c} + \mathrm{Da}\, c' = \frac{\partial^2 \bar{c}}{\partial x^2} + \frac{\partial^2 c'}{\partial x^2} + \frac{\partial^2 c'}{\partial z^2}, \tag{19}$$

$$\bar{c}(x, t = 0) + c'(x, z, t = 0) = 0, \tag{20}$$

$$\bar{c}(x = 0, t) + c'(x = 0, z, t) = 0, \tag{21}$$

$$\frac{\partial \bar{c}(x = L, t)}{\partial x} + \frac{\partial c'(x = L, z, t)}{\partial x} = 0, \tag{22}$$

$$\bar{c}(x, t) + c'(x, z = 0, t) = 1, \tag{23}$$

and

$$\frac{\partial c'(x, z = 1, t)}{\partial z} = 0. \tag{24}$$

The cross-sectional average of Eq. (19) using Eq. (15), along with the aid of Eqs. (17) and (24) gives

$$\frac{\partial \bar{c}}{\partial t} + \mathrm{Pe}\, \frac{\partial \bar{c}}{\partial x} + \mathrm{Pe}\, \overline{u(z)\frac{\partial c'}{\partial x}} + \mathrm{Da}\, \bar{c} = \frac{\partial^2 \bar{c}}{\partial x^2} - \frac{\partial c'(x, z = 0, t)}{\partial z}. \tag{25}$$

Subtracting Eq. (25) from Eq. (19) results in

$$\frac{\partial c'}{\partial t} + \mathrm{Pe}\,[u(z) - 1]\frac{\partial \bar{c}}{\partial x} + \mathrm{Pe}\, u(z)\frac{\partial c'}{\partial x} - \mathrm{Pe}\, \overline{u(z)\frac{\partial c'}{\partial x}} + \mathrm{Da}\, c' = \frac{\partial^2 c'}{\partial x^2} + \frac{\partial^2 c'}{\partial z^2} + \frac{\partial c'(x, z = 0, t)}{\partial z}. \tag{26}$$

Equation (26), which is exact, can be reduced to Eq. (27) if the three assumptions adopted by Taylor [21] and Fischer *et al.* [42], including $\partial c'/\partial t \approx 0$ for a timescale on the order of magnitude of the diffusion time across the liquid phase (δ^2/D), $\mathrm{Pe}\, u(z)\partial c'/\partial x \approx \mathrm{Pe}\, \overline{u(z)\partial c'/\partial x}$ for slowly varying fluctuation components, and $\mathrm{Pe}\,[u(z) - 1]\partial \bar{c}/\partial x \gg \partial^2 c'/\partial x^2$ for a controlled gas solute transport by the longitudinal advection and transversal diffusion, along with Eq. (6), are taken into consideration here:

$$\mathrm{Pe}\left(\frac{1}{2} - \frac{3}{2}z^2\right)\frac{\partial \bar{c}}{\partial x} - \frac{\partial c'(x, z = 0, t)}{\partial z} = \frac{\partial^2 c'}{\partial z^2} - \mathrm{Da}\, c'. \tag{27}$$

Equation (27) is an inhomogeneous, second-order linear ordinary differential equation, which can lead to the following expression for c' when subjected to Eqs. (12) and (17) to find the two integration constants:

$$c' = \mathrm{Pe}\left(-\frac{3\cosh(\sqrt{\mathrm{Da}}z)}{\mathrm{Da}^{3/2}\sinh(\sqrt{\mathrm{Da}})} + \frac{(3z^2 - 1)\mathrm{Da} + 6}{2\mathrm{Da}^2}\right)\frac{\partial \bar{c}}{\partial x} + \left(\frac{\sinh(\sqrt{\mathrm{Da}}z)}{\sqrt{\mathrm{Da}}} - \frac{\cosh(\sqrt{\mathrm{Da}}z)}{\sqrt{\mathrm{Da}}\tanh(\sqrt{\mathrm{Da}})} + \frac{1}{\mathrm{Da}}\right) \times \frac{\partial c'(x, z = 0, t)}{\partial z}. \tag{28}$$

Using Eq. (28), the expression for $\partial c'/\partial x$, which is needed to determine $\overline{u(z)\partial c'/\partial x}$ in Eq. (25) and to close the formulation, can be obtained as follows:

$$\frac{\partial c'}{\partial x} = \mathrm{Pe}\left(-\frac{3\cosh(\sqrt{\mathrm{Da}}z)}{\mathrm{Da}^{3/2}\sinh(\sqrt{\mathrm{Da}})} + \frac{(3z^2 - 1)\mathrm{Da} + 6}{2\mathrm{Da}^2}\right)\frac{\partial^2 \bar{c}}{\partial x^2} + \left(\frac{\sinh(\sqrt{\mathrm{Da}}z)}{\sqrt{\mathrm{Da}}} - \frac{\cosh(\sqrt{\mathrm{Da}}z)}{\sqrt{\mathrm{Da}}\tanh(\sqrt{\mathrm{Da}})} + \frac{1}{\mathrm{Da}}\right) \times \frac{\partial^2 c'(x, z = 0, t)}{\partial z \partial x}. \tag{29}$$

Therefore, the cross-sectional average of the product of Eqs. (6) and (29) gives

$$\overline{u(z)\frac{\partial c'}{\partial x}} = \int_0^1 u(z)\frac{\partial c'}{\partial x}dz = \Omega\mathrm{Pe}\frac{\partial^2 \bar{c}}{\partial x^2} + \Psi\frac{\partial^2 c'(x, z = 0, t)}{\partial z \partial x}, \tag{30}$$

where the constants Ω and Ψ are defined as

$$\Omega = -\frac{9}{\mathrm{Da}^{5/2}\tanh(\sqrt{\mathrm{Da}})} + \frac{9}{\mathrm{Da}^3} + \frac{3}{\mathrm{Da}^2} - \frac{1}{5\mathrm{Da}} \tag{31}$$

and

$$\Psi = \frac{3}{\mathrm{Da}^2} - \frac{1}{2\mathrm{Da}} - \frac{3}{\mathrm{Da}^{3/2}\sinh(\sqrt{\mathrm{Da}})}. \tag{32}$$

Replacing for $\overline{u(z)\partial c'/\partial x}$ in Eq. (25) from Eq. (30) results in

$$\frac{\partial \bar{c}}{\partial t} + \mathrm{Pe}\,\frac{\partial \bar{c}}{\partial x} + \mathrm{Da}\,\bar{c} = (1 - \Omega \mathrm{Pe}^2)\frac{\partial^2 \bar{c}}{\partial x^2} - \frac{\partial c'(x, z = 0, t)}{\partial z} - \Psi \mathrm{Pe}\frac{\partial^2 c'(x, z = 0, t)}{\partial z \partial x}. \tag{33}$$

The interface between the gas and liquid causes the last two derivatives on the right-hand side of Eq. (33) to be nonzero; therefore, the appropriate expressions need to be obtained to close the problem. First, Eq. (28) is evaluated at $z = 0$ and combined with Eq. (23) to replace the first derivative with the expression

$$\frac{\partial c'(x, z = 0, t)}{\partial z} = \frac{1}{\Phi}(1 - \bar{c}) - \frac{\Psi}{\Phi}\mathrm{Pe}\frac{\partial \bar{c}}{\partial x}, \tag{34}$$

where the constant Φ is defined as

$$\Phi = -\frac{1}{\sqrt{\mathrm{Da}}\tanh(\sqrt{\mathrm{Da}})} + \frac{1}{\mathrm{Da}}. \tag{35}$$

Second, Eq. (34) needs to be differentiated with respect to x to replace the second derivative with the following expression:

$$\frac{\partial^2 c'(x, z = 0, t)}{\partial z \partial x} = -\frac{1}{\Phi}\frac{\partial \bar{c}}{\partial x} - \frac{\Psi}{\Phi}\mathrm{Pe}\frac{\partial^2 \bar{c}}{\partial x^2}. \tag{36}$$

Substituting Eqs. (34) and (36) into Eq. (33) leads to the extended reduced-order model of advection-dispersion-reaction solute transport due to a laminar flow of a viscous incompressible liquid with a gas absorption on an inclined surface,

$$\frac{\partial \bar{c}}{\partial t} = K\frac{\partial^2 \bar{c}}{\partial x^2} - V\frac{\partial \bar{c}}{\partial x} - \lambda \bar{c} + \omega, \tag{37}$$

where the constants K, V, λ, and ω are defined as

$$K = 1 + \left(-\Omega + \frac{\Psi^2}{\Phi}\right)\mathrm{Pe}^2, \tag{38}$$

$$V = \left(1 - \frac{2\Psi}{\Phi}\right)\mathrm{Pe}, \tag{39}$$

$$\lambda = \left(1 - \frac{1}{\Phi \mathrm{Da}}\right)\mathrm{Da}, \tag{40}$$

and

$$\omega = -\frac{1}{\Phi}. \tag{41}$$

It is worth noting that the last two terms, λ and ω, are the equivalent reaction constant and source term. The term λ accounts for the reaction rate of the gaseous solute in the liquid phase, while the source term, ω, accounts for the gas-liquid interface.

For a special case, in the absence of gas absorption and a closed boundary at $z = 0$, the gas solute concentration gradient (or flux) will be zero, and these two derivatives on the right-hand side of Eq. (33) vanish. As a result, the nondimensional dispersion coefficient of $K = 1 - \Omega \mathrm{Pe}^2$ for the advection-dispersion-reaction solute transport is obtained. As the Damköhler number approaches zero ($\mathrm{Da} \to 0$), K becomes equal to $1 + (2\mathrm{Pe}^2/105)$ [43]. The detailed derivation of the dispersion for gas absorption into a liquid phase without reaction on an inclined surface is presented in the Appendix.

Equations (38) and (39) stand for dispersion and advection coefficients, respectively.

Equation (37), subject to the following initial and boundary conditions, can be solved to obtain the early-time solution of the cross-sectional average concentration:

$$\bar{c}(x, t = 0) = 0, \tag{42}$$

$$\bar{c}(x = 0, t) = 0, \tag{43}$$

and

$$\frac{\partial \bar{c}(x \to \infty, t)}{\partial x} = 0. \tag{44}$$

Equations (42)–(44) are found by the cross-sectional average of Eqs. (20)–(22), where $x = L$ is replaced by $x \to \infty$, using Eq. (15) along with the aid of Eq. (17).

Taking the Laplace transform with respect to t from Eqs. (37), (43), and (44) using Eq. (42) gives

$$K\frac{d^2\tilde{\bar{c}}}{dx^2} - V\frac{d\tilde{\bar{c}}}{dx} - (\lambda + s)\tilde{\bar{c}} = -\frac{\omega}{s}, \tag{45}$$

$$\tilde{\bar{c}}(x = 0, s) = 0, \tag{46}$$

and

$$\frac{\partial \tilde{\bar{c}}(x \to \infty, s)}{\partial x} = 0, \tag{47}$$

where the nondimensional cross-sectional average gas concentration in the Laplace domain, $\tilde{\bar{c}}$, is defined as

$$\tilde{\bar{c}}(x, s) = \ell_t\{\bar{c}(x, t)\} = \int_0^\infty e^{-st}\bar{c}(x, t)dt, \tag{48}$$

in which ℓ_t is the Laplace transform operator with respect to t, and s is the Laplace variable.

Equation (45) is an inhomogeneous, seconder-order linear ordinary differential equation, which can lead to the following expression for $\tilde{\bar{c}}$ if it is subjected to Eqs. (46) and (47) to find the two integration constants:

$$\tilde{\bar{c}}(x, s) = \frac{\omega}{s(\lambda + s)}\left(1 - e^{\left[\frac{V}{2K} - \sqrt{\left(\frac{V}{2K}\right)^2 + \frac{1}{K}(s+\lambda)}\right]x}\right). \tag{49}$$

This solution, Eq. (49), can be inverted to a time domain solution using the shift theorem [44] as given by

$$\bar{c}(x, t) = \frac{\omega}{\lambda}(1 - e^{-\lambda t}) - \frac{1}{2}\int_0^t \omega e^{-\lambda(t-\tau)}e^{\left(\frac{V}{2K}\right)x} \times \left\{e^{-\sqrt{\frac{\alpha}{K}}x}\mathrm{erfc}\left(\frac{x}{2\sqrt{K\tau}} - \sqrt{\alpha\tau}\right) + e^{\sqrt{\frac{\alpha}{K}}x}\mathrm{erfc}\left(\frac{x}{2\sqrt{K\tau}} + \sqrt{\alpha\tau}\right)\right\}d\tau, \tag{50}$$

where τ is the integral variable and the constant α is defined as

$$\alpha = \left(\frac{V}{2\sqrt{K}}\right)^2 + \lambda. \tag{51}$$

Equation (37), subject to Eqs. (42) and (43) and the following boundary condition, can be solved to find $\bar{c}$ for a domain of finite length L:

$$\frac{\partial \bar{c}(x = L, t)}{\partial x} = 0. \tag{52}$$

Equation (52) is found by the cross-sectional average of Eq. (22) using Eq. (15), along with the aid of Eq. (17).

Using the separation of variables, Eq. (37), subject to Eqs. (42), (43), and (52), gives the analytical solution

$$\bar{c}(x,t) = \frac{\omega}{\lambda}\left(1 - \frac{r_2 e^{r_2 L} e^{r1x} - r_1 e^{r_1 L} e^{r_2 x}}{r_2 e^{r_2 L} - r_1 e^{r_1 L}}\right) + \sum_{n=1}^{\infty} c_n e^{-(\frac{V}{2K})x} \sin(\sqrt{\mu_n} x) e^{-(\alpha+\mu_n K)t}, \quad (53)$$

where r_1 and r_2 are the real distinct roots of the characteristic polynomial equation $Kr^2 - Vr - \lambda = 0$, which can be obtained as

$$r_1, r_2 = \frac{V}{2K} \pm \sqrt{\frac{\alpha}{K}}, \quad (54)$$

μ_n are the roots of the transcendental equation

$$\left(\frac{V}{2K}\right) \tan\sqrt{\mu_n} + \sqrt{\mu_n} = 0, \quad n = 1, 2, 3, \ldots, \infty, \quad (55)$$

and c_n is expressed by

$$c_n = \frac{4\omega\sqrt{\mu_n}}{\lambda\,[2L\sqrt{\mu_n} - \sin(2\sqrt{\mu_n}L)]} \times \int_0^L \left(\frac{r_2 e^{r_2 L} e^{r_1 x} - r_1 e^{r_1 L} e^{r_2 x}}{r_2 e^{r_2 L} - r_1 e^{r_1 L}} - 1\right) e^{-(\frac{V}{2K})x} \times \sin(\sqrt{\mu_n} x) dx. \quad (56)$$

The steady-state form of Eq. (37) turns to

$$K\frac{d^2\bar{c}}{dx^2} - V\frac{d\bar{c}}{dx} - \lambda\bar{c} = -\omega. \quad (57)$$

Equation (57) is an inhomogeneous, second-order linear ordinary differential equation, which can lead to the following expression for $\bar{c}$ when subjected to Eqs. (43) and (52) to find the two integration constants:

$$\bar{c}(x) = \frac{\omega}{\lambda}\left(1 - \frac{r_2 e^{r_2 L} e^{r_1 x} - r_1 e^{r_1 L} e^{r_2 x}}{r_2 e^{r_2 L} - r_1 e^{r_1 L}}\right). \quad (58)$$

The local Sherwood number, Sh_x, is defined as the ratio of the gas solute mass flux to the pure diffusive flux at the interface, as given by

$$\mathrm{Sh}_x = -\frac{1}{1-\bar{c}}\frac{\partial c(x, z=0, t)}{\partial z} = -\frac{1}{1-\bar{c}}\frac{\partial c'(x, z=0, t)}{\partial z}. \quad (59)$$

The combination of Eqs. (34), (58), and (59) results in

$$\mathrm{Sh}_x = -\frac{1}{\Phi} + \frac{\Psi}{\Phi}\frac{\mathrm{Pe}}{\left(1 - \frac{\omega}{\lambda}\left(1 - \frac{r_2 e^{r_2 L} e^{r_1 x} - r_1 e^{r_1 L} e^{r_2 x}}{r_2 e^{r_2 L} - r_1 e^{r_1 L}}\right)\right)}\frac{\omega}{\lambda} r_1 r_2 \times \left(\frac{e^{r_1 L} e^{r_2 x} - e^{r_2 L} e^{r_1 x}}{r_2 e^{r_2 L} - r_1 e^{r_1 L}}\right). \quad (60)$$

The overall Sherwood number can be obtained by averaging Sh_x, Eq. (60), along the interface:

$$\mathrm{Sh} = \frac{1}{L}\int_0^L \mathrm{Sh}_x dx. \quad (61)$$

The integral in Eq. (61) has been evaluated numerically.

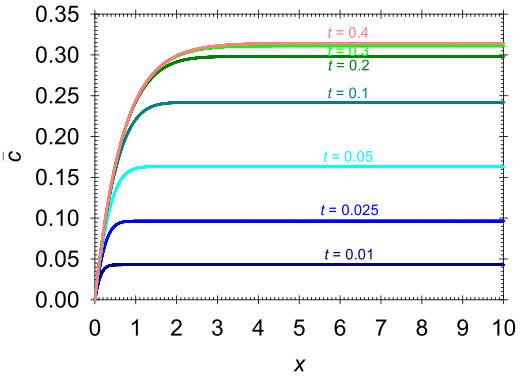

FIG. 2. The transient cross-sectional average concentration $\bar{c}$ along the surface x for several times at Da = 10 and Pe = 10.

IV. RESULTS AND DISCUSSION

Figure 2 depicts the transient behavior of the cross-sectional average concentration for Da = 10 and Pe = 10 at various time intervals using Eq. (50). The findings indicate that the concentration profile attains a steady-state solution at $t \sim 0.3$. Furthermore, the results suggest that the concentration reaches a plateau beyond $L \sim 2$, implying that the longitudinal concentration gradients can be ignored. Therefore, the system can be considered lumped, and the plateaued transient concentrations can be obtained using the solution to the following first-order linear ordinary differential equation:

$$\frac{d\bar{c}}{dt} = -\lambda\bar{c} + \omega. \quad (62)$$

Equation (62) subject to $\bar{c}(0) = 0$ gives

$$\bar{c}(t) = \frac{\omega}{\lambda}(1 - e^{-\lambda t}). \quad (63)$$

The results indicate that steady-state plateaued concentrations can be expressed as $\bar{c}_{ss} = \omega/\lambda$.

Figure 3 shows the steady-state cross-sectional average concentration profiles for various Peclet and Damköhler numbers using Eq. (58). As shown, a higher Damköhler number leads to the rapid absorption of the gas solute at the gas-liquid interface and a significant decrease in its concentration throughout the domain. The concentration profiles also reveal that at high Peclet numbers, the system is flooded with fresh liquid devoid of the solute, leading to a substantial decrease in solute concentration along the domain. While the effect of the Peclet number is not evident at high Damköhler numbers, its effect becomes more prominent at low Damköhler numbers.

Figure 4(a) and 4(b) shows K (dispersion coefficient) and V (advection coefficient) as a function of Da, respectively, for different Peclet numbers, $0.01 \leqslant \mathrm{Pe} \leqslant 10^4$, obtained using Eqs. (38) and (39). The reaction term λ and source term ω versus Da are also shown in Fig. 4(c) and 4(d), respectively, obtained using Eqs. (40) and (41). It is revealed from Fig. 4(a) that for $\mathrm{Pe} \leqslant 1$, the dispersion remains around unity ($K \approx 1$) as the Damköhler number is increased. This implies that the transport by dispersion is negligible. For $\mathrm{Pe} > 1$, as expected, the dispersion increases by increasing the Peclet number. However, when $\mathrm{Da} \leqslant 1$, the transport is primarily governed by diffusion and advection, with its dependence on Da being nearly negligible. The limiting value of the dis-

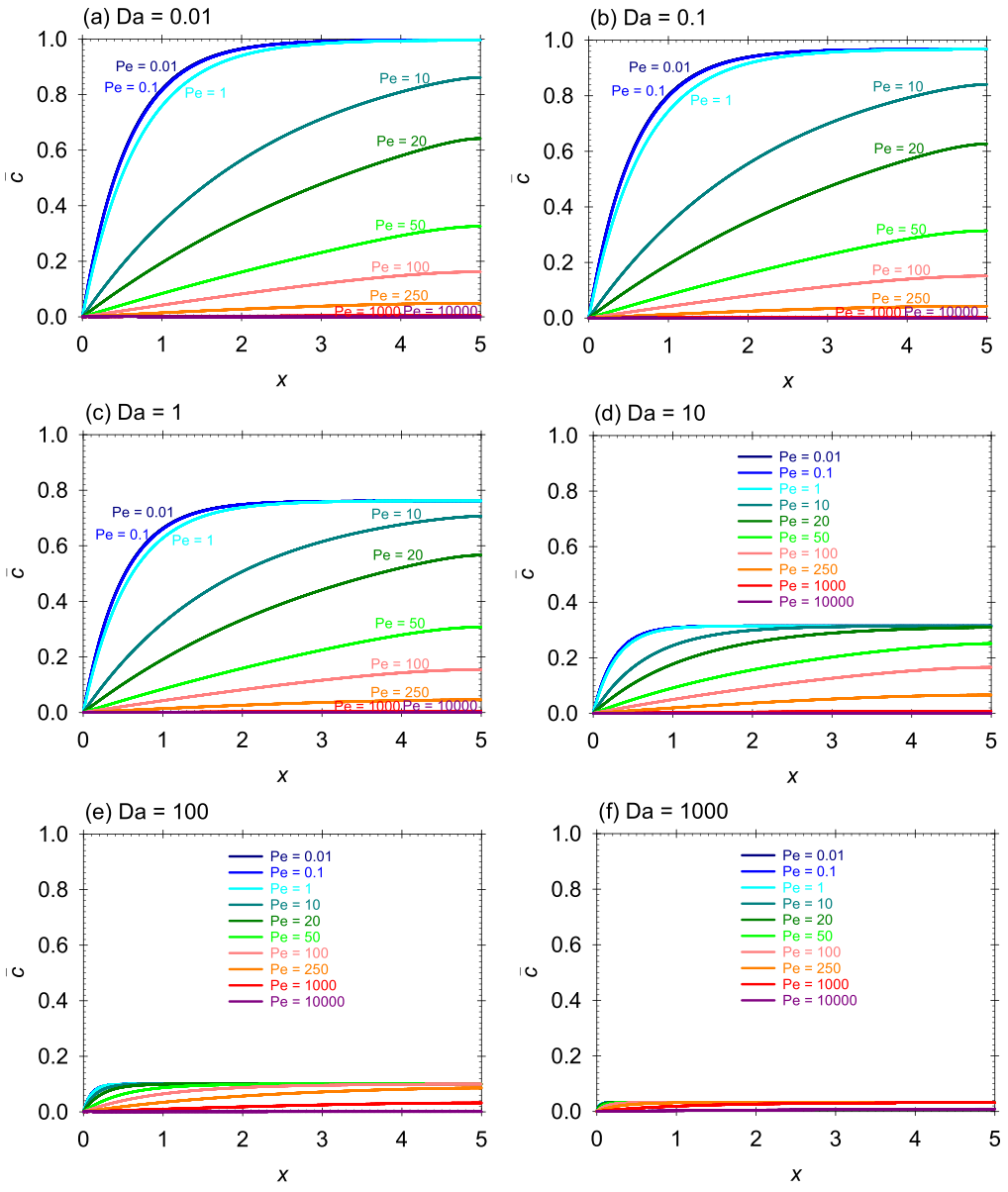

FIG. 3. The steady-state cross-sectional average concentration $\bar{c}$ with respect to the distance along the surface x for several Damköhler numbers, where Da = (a) 0.01, (b) 0.1, (c), 1, (d) 10, (e) 100, and (f) 1000 at different Peclet numbers, $0.01 \leqslant \mathrm{Pe} \leqslant 10\,000$.

persion for each Peclet number in the absence of absorption can be obtained using Eq. (38) when $\mathrm{Da} \to 0$, as given by $K = 1 + (99\mathrm{Pe}^2/11\,200)$, which is also confirmed from the solution obtained for this special case given by Eq. (A13). For $\mathrm{Da} > 1$, the absorption process becomes significant, leading to a reduction in dispersion as the solute gas is absorbed into the liquid phase. Finally, as Da approaches infinity ($\mathrm{Da} \to \infty$), the dispersion tends to unity, indicating insignificant transport by dispersion, which can be deduced from Eq. (38). When the Damköhler number approaches infinity, the solute is consumed nearly instantaneously at the gas-liquid interface. Consequently, this results in the complete absorption of the solute by the liquid, leading to its absence within the liquid phase. This can also be inferred from Eqs. (31) and (32), where both Ω and Ψ tend to approach zero as the Damköhler number approaches infinity.

The results depicted in Fig. 4(b) indicate that, as anticipated, advection intensifies with an increase in the Peclet number. The results also inferred that, initially, advection remains constant. Subsequently, it gradually increases and eventually stabilizes for each Peclet number value as the Damköhler number increases. For the case of a very small Da, the limiting value of the advection can be found by applying Eq. (39) when $\mathrm{Da} \to 0$, as $V = 13\mathrm{Pe}/20$. The results suggest that the upscaled advection is approximately 13/20 of the actual advection when $\mathrm{Da} \to 0$. In the scenario of a large Damköhler number ($\mathrm{Da} \to \infty$) Ψ, as indicated by Eq. (32), tends to approach zero. This reduces Eq. (39) to $V = \mathrm{Pe}$. For this limiting case, the nonabsorbing liquid recovers the same result, as shown by Eq. (A14). In summary, the advection increases from $13\mathrm{Pe}/20$ to Pe when the Damköhler number varies from zero to infinity.

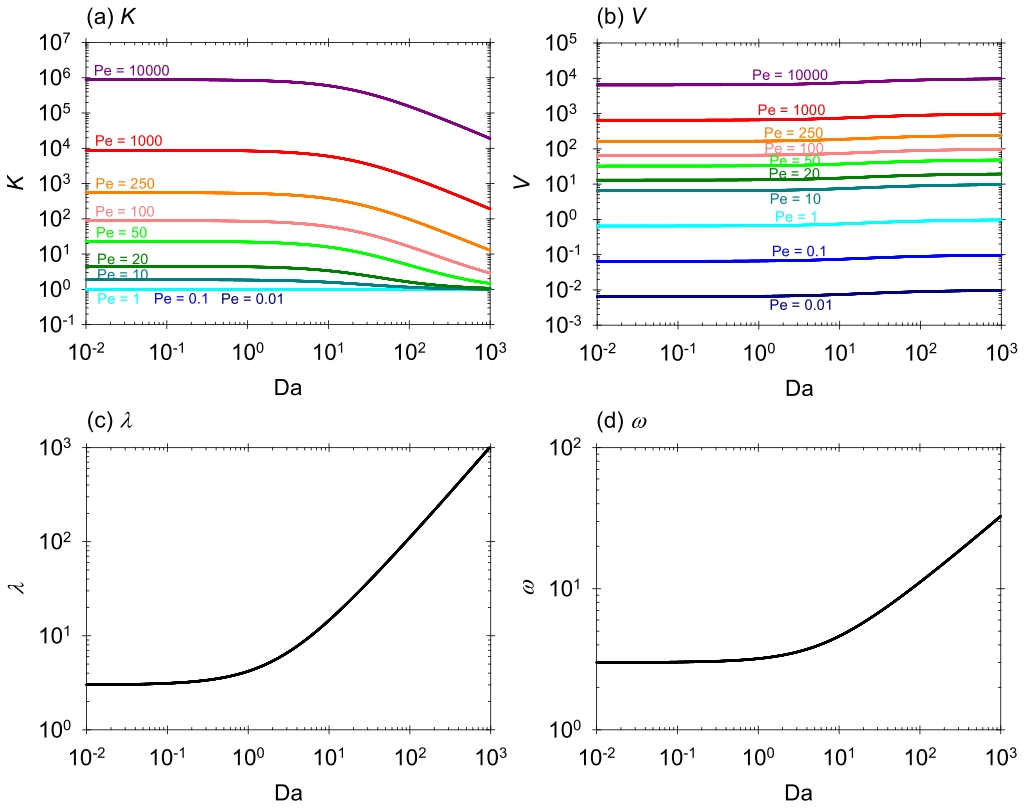

FIG. 4. (a) K (dispersion coefficient) and (b) V (advection coefficient) as a function of the Da for different Pe, $0.01 \leqslant \mathrm{Pe} \leqslant 10\,000$, and (c) λ and (d) ω versus Da.

Figure 4(c) and 4(d) shows the upscaled absorption coefficient λ and the source term ω, respectively. The upscaled absorption coefficient represents the reduced-order gas absorption in the liquid, and the source term originates from the gas-liquid interface boundary condition. Both the upscaled absorption coefficient and the source term are independent of the Peclet number and only function of the Damköhler number. The results indicate that the values of λ and ω remain unaffected by the Damköhler number when $\mathrm{Da} \leqslant 0.1$. However, beyond this threshold, both λ and ω increase with the increment of Da. For low Damköhler numbers ($\mathrm{Da} \leqslant 0.1$), $\lambda = \omega = 3$, which can be inferred from Eqs. (40) and (41) when $\mathrm{Da} \to 0$. For the special case of a nonabsorbing liquid, Eqs. (A15) and (A16) recover the same solutions. The upscaled absorption coefficient represents first-order absorption kinetics while the source term represents a zero-order kinetic, and the value of λ exceeds the value of ω for $\mathrm{Da} > 0.1$.

Figure 5(a) and 5(b) illustrates the relationship between the overall Sh and the Da obtained using Eq. (61), for the respective ranges of $0.01 \leqslant \mathrm{Da} \leqslant 1000$ and $0.01 \leqslant \mathrm{Da} \leqslant 10$. The figures are plotted for various Pe ranging from 0.01 to 10 000. Three different regions can be identified in Fig. 5(a). In the first region ($\mathrm{Da} \leqslant 1$), for each Peclet number, the Sherwood number exhibits minimal variations with Da, indicating that Sh primarily depends on the Peclet number rather than the Damköhler number. In this region, the Sherwood number demonstrates a nonmonotonic behavior with respect to the Peclet number. Therefore, the first region is controlled by advection.

In the second region ($1 < \mathrm{Da} < 10$), Sh varies with both Da and Pe. Although the Sherwood number demonstrates a nonmonotonic behavior in relation to Pe, it increases as the Damköhler number increases. Consequently, the second region is influenced by both advection and absorption, making it Peclet and Damköhler dependent. The inset plot in Fig. 5(b) also illustrates Sh as a function of Pe for $\mathrm{Da} = 0$, 0.01, 0.1, and 1. In the first two regions, for all Damköhler numbers, the relationship between the Sherwood number and the Peclet number exhibits a bell-shaped (or Gaussian) behavior. This indicates that there exists a specific Peclet number for the first two regions at which the mass transfer can be maximized by controlling the advective transport, Pe.

In the third region ($\mathrm{Da} \geqslant 10$), the Sherwood number solely depends on the Damköhler number, and it tends to increase as the Damköhler number increases. Thus, in the third region, the behavior is primarily governed by absorption and is independent of advection effects. The scaling relation between Sherwood and Damköhler numbers can be found as $\mathrm{Sh} \sim \mathrm{Da}^{1/2}$, suggesting that, in the third region, mass transfer is directly proportional to the thickness of the liquid and the square root of absorption kinetics while being inversely proportional to the molecular diffusion of gas into the liquid.

V. CONCLUSION

The upscaling of dispersion in gas-liquid absorption on an inclined surface is studied. The Taylor-Aris dispersion theory, along with Reynolds decomposition and cross-sectional

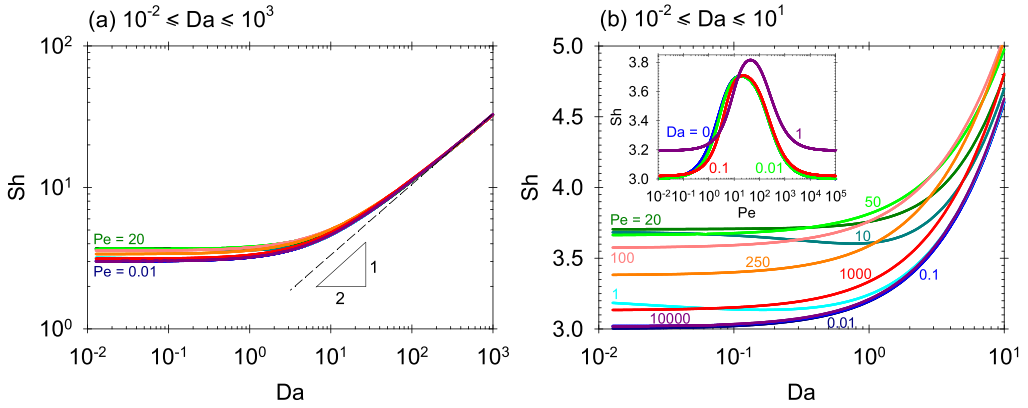

FIG. 5. The overall Sh versus the Da for (a) $0.01 \leqslant Da \leqslant 1000$ and (b) $0.01 \leqslant Da \leqslant 10$. Inset: Sh as a function of Pe for Da = 0, 0.01, 0.1, and 1.

averaging, is extended to develop the reduced-order model of advection-dispersion-reaction solute transport. The model specifically considers the laminar flow of a viscous incompressible liquid on an inclined surface with gas absorption occurring at the gas-liquid interface. The reduced-order model obtained allows evaluation of the upscaled dispersion, advection, absorption, and interface boundary condition as functions of the system's dimensionless groups—namely, the Peclet and Damköhler numbers.

The evaluation of the resultant upscaled dispersion coefficients reveals that for a specified Peclet number, gas absorption leads to a reduction in the dispersion coefficient. In the absence of absorption, the dispersion coefficient as a function of the Peclet number can be expressed as $K = 1 + (99\mathrm{Pe}^2/11\,200)$. However, in an absorption-dominant system, the dispersion coefficient approaches unity, indicating that transport is primarily driven by pure diffusion. As expected, the dispersion is found to be an increasing function of the Peclet number. In the absence of absorption, the upscaled advection coefficient as a function of the Peclet number can be expressed as $13\mathrm{Pe}/20$. This finding implies that the upscaled advection coefficient is a fraction of the coefficient observed in the detailed two-dimensional model. On the other hand, in an absorption-dominant system, the advection coefficient approaches the Peclet number, indicating that the advection coefficient retains its original value of the detailed two-dimensional model. The upscaled reaction kinetics were found to be an increasing function of the Damköhler number. In the limit of no absorption, the upscaled kinetics approach a constant value of $\lambda = 3$. The gas-liquid interface boundary condition appeared as zero-order kinetics in the upscaled model, which is shown to be an increasing function of the Damköhler number. The zero-order kinetics approach a constant value of $\omega = 3$ for a nonabsorbing system. The results suggest that the zero-order kinetics constant is lower than the first-order kinetics constant for all Da values greater than 0.1.

The upscaled model was solved analytically, and the mass transfer between gas and liquid was evaluated. The results for the overall Sherwood number identify three different regions: (i) advection dominant, (ii) transition, and (iii) absorption dominant. The scaling relationship between the Sherwood number and the Damköhler number for the third region was found to follow $\mathrm{Sh} \sim \mathrm{Da}^{1/2}$. It is also revealed that the Sherwood number versus the Peclet number for the first two regions exhibits a bell-shaped (or Gaussian) behavior, suggesting that there is an optimal Peclet number where the mass transfer can be maximized by manipulating the advective transport.

The model and the insight presented in this work find potential applications in various industrial separation processes. One notable example is the absorption of carbon dioxide from gaseous streams. The ability to predict and optimize the mass transfer accurately in such processes is crucial for enhancing their efficiency.

ACKNOWLEDGMENTS

M.D. is gratefully appreciative of the support from the Department of Energy and Petroleum Engineering in the College of Engineering and Physical Sciences at the University of Wyoming. H.H. acknowledges the support from the Department of Chemical and Petroleum Engineering in the Schulich School of Engineering at the University of Calgary.

APPENDIX: DISPERSION FOR GAS ABSORPTION INTO A LIQUID PHASE WITHOUT REACTION ON AN INCLINED SURFACE

The mass balance leads to the following unsteady two-dimensional advective-diffusive equation for the nondimensional concentration of gas solute in the liquid phase, $c(x, z, t)$:

$$\frac{\partial c}{\partial t} + \mathrm{Pe}\, u(z)\frac{\partial c}{\partial x} = \frac{\partial^2 c}{\partial x^2} + \frac{\partial^2 c}{\partial z^2}. \tag{A1}$$

Replacing for c in Eq. (A1) from Eq. (13) leads to

$$\frac{\partial \bar{c}}{\partial t} + \frac{\partial c'}{\partial t} + \mathrm{Pe}\, u(z)\frac{\partial \bar{c}}{\partial x} + \mathrm{Pe}\, u(z)\frac{\partial c'}{\partial x} = \frac{\partial^2 \bar{c}}{\partial x^2} + \frac{\partial^2 c'}{\partial x^2} + \frac{\partial^2 c'}{\partial z^2}. \tag{A2}$$

The cross-sectional average of Eq. (A2) using Eq. (15) along with the aid of Eqs. (17) and (24) gives

$$\frac{\partial \bar{c}}{\partial t} + \mathrm{Pe}\,\frac{\partial \bar{c}}{\partial x} + \mathrm{Pe}\,\overline{u(z)\frac{\partial c'}{\partial x}} = \frac{\partial^2 \bar{c}}{\partial x^2} - \frac{\partial c'(x, z = 0, t)}{\partial z}. \tag{A3}$$

Subtracting Eq. (A3) from Eq. (A2) results in

$$\frac{\partial c'}{\partial t} + \mathrm{Pe}\,[u(z)-1]\frac{\partial \bar{c}}{\partial x} + \mathrm{Pe}\,u(z)\frac{\partial c'}{\partial x} - \mathrm{Pe}\,\overline{u(z)\frac{\partial c'}{\partial x}} = \frac{\partial^2 c'}{\partial x^2} + \frac{\partial^2 c'}{\partial z^2} + \frac{\partial c'(x, z=0, t)}{\partial z}. \tag{A4}$$

Equation (A4), which is exact, can be reduced to Equation (A5) if the three assumptions adopted by Taylor [21] and Fischer *et al.* [42], along with Eq. (6) are taken into consideration here:

$$\mathrm{Pe}\left(\frac{1}{2} - \frac{3}{2}z^2\right)\frac{\partial \bar{c}}{\partial x} - \frac{\partial c'(x, z=0, t)}{\partial z} = \frac{\partial^2 c'}{\partial z^2}. \tag{A5}$$

Equation (A5) is an inhomogeneous, second-order linear ordinary differential equation, which can lead to the following expression for c' if it is subjected to Eqs. (12) and (17) to find the two integration constants:

$$c' = \mathrm{Pe}\left(-\frac{7}{120} - \frac{1}{8}z^4 + \frac{1}{4}z^2\right)\frac{\partial \bar{c}}{\partial x} + \left(z - \frac{1}{3} - \frac{1}{2}z^2\right)\frac{\partial c'(x, z=0, t)}{\partial z}. \tag{A6}$$

Using Eq. (A6), the expression for $\partial c'/\partial x$, which is needed to determine $\overline{u(z)\partial c'/\partial x}$ in Eq. (A3) and to close the modeling, can be obtained as follows:

$$\frac{\partial c'}{\partial x} = \mathrm{Pe}\left(-\frac{7}{120} - \frac{1}{8}z^4 + \frac{1}{4}z^2\right)\frac{\partial^2 \bar{c}}{\partial x^2} + \left(z - \frac{1}{3} - \frac{1}{2}z^2\right)\frac{\partial^2 c'(x, z=0, t)}{\partial z \partial x}. \tag{A7}$$

Therefore, the cross-sectional average of the product of Eqs. (6) and (A7) gives

$$\overline{u(z)\frac{\partial c'}{\partial x}} = \int_0^1 u(z)\frac{\partial c'}{\partial x}dz = -\frac{2}{105}\mathrm{Pe}\frac{\partial^2 \bar{c}}{\partial x^2} - \frac{7}{120}\frac{\partial^2 c'(x, z=0, t)}{\partial z \partial x}. \tag{A8}$$

Replacing for $\overline{u(z)\partial c'/\partial x}$ in Eq. (A3) from Eq. (A8) results in

$$\frac{\partial \bar{c}}{\partial t} + \mathrm{Pe}\,\frac{\partial \bar{c}}{\partial x} = \left(1 + \frac{2}{105}\mathrm{Pe}^2\right)\frac{\partial^2 \bar{c}}{\partial x^2} - \frac{\partial c'(x, z=0, t)}{\partial z} + \frac{7}{120}\mathrm{Pe}\frac{\partial^2 c'(x, z=0, t)}{\partial z \partial x}. \tag{A9}$$

The interface between the gas and liquid causes the last two derivatives on the right-hand side of Eq. (A9) to be nonzero; therefore, the appropriate expressions need to be obtained to replace them. If there is no gas absorption and the liquid is bounded at $z = 0$, the gas concentration gradient (or gas flux) will be zero, and these two derivatives will vanish. As a result, the advection-dispersion solute transport due to a laminar flow of a viscous incompressible liquid without gas absorption, including the nondimensional dispersion coefficient of $K = 1 + (2\mathrm{Pe}^2/105)$, will be achieved. To replace the first derivative with the appropriate expression, Eq. (A6) is determined at $z = 0$ and combined with Eq. (23):

$$\frac{\partial c'(x, z=0, t)}{\partial z} = -3(1-\bar{c}) - \frac{7}{40}\mathrm{Pe}\frac{\partial \bar{c}}{\partial x}. \tag{A10}$$

To replace the second derivative by the appropriate expression, Eq. (A10) needs to be differentiated with respect to x:

$$\frac{\partial^2 c'(x, z=0, t)}{\partial z \partial x} = 3\frac{\partial \bar{c}}{\partial x} - \frac{7}{40}\mathrm{Pe}\frac{\partial^2 \bar{c}}{\partial x^2}. \tag{A11}$$

Substituting Eqs. (A10) and (A11) into Eq. (A9) leads to the extended reduced-order model of advection-dispersion solute transport due to a laminar flow of a viscous incompressible liquid with gas absorption on an inclined surface,

$$\frac{\partial \bar{c}}{\partial t} = K\frac{\partial^2 \bar{c}}{\partial x^2} - V\frac{\partial \bar{c}}{\partial x} - \lambda\bar{c} + \omega, \tag{A12}$$

where the constants K, V, λ, and ω are defined as

$$K = 1 + \frac{99}{11\,200}\mathrm{Pe}^2, \tag{A13}$$

$$V = \frac{13}{20}\mathrm{Pe}, \tag{A14}$$

$$\lambda = 3, \tag{A15}$$

and

$$\omega = 3. \tag{A16}$$

Equation (A12) subject to Eqs. (42)–(44) can be solved to obtain the early-time solution of the cross-sectional average concentration. Taking the Laplace transform with respect to t from Eq. (A12) using Eq. (42) gives

$$K\frac{d^2\tilde{\bar{c}}}{dx^2} - V\frac{d\tilde{\bar{c}}}{dx} - (\lambda + s)\tilde{\bar{c}} = -\frac{\omega}{s}. \tag{A17}$$

Equation (A17) is an inhomogeneous second-order linear ordinary differential equation, which can lead to the following expression for $\tilde{\bar{c}}$ if it is subjected to Eqs. (46) and (47) to find the two integration constants:

$$\tilde{\bar{c}}(x, s) = \frac{\omega}{s(\lambda + s)}\left(1 - e^{\left[\frac{V}{2K} - \sqrt{\left(\frac{V}{2K}\right)^2 + \frac{1}{K}(s+\lambda)}\right]x}\right). \tag{A18}$$

This solution, Eq. (A18), can be inverted to a time domain solution using the shift theorem [44] as given by

$$\bar{c}(x, t) = 1 - e^{-\lambda t} - \int_0^t \omega e^{-\lambda(t-\tau)}\frac{1}{2}e^{\left(\frac{V}{2K}\right)x} \times \left\{e^{-\sqrt{\frac{\alpha}{K}}x}\mathrm{erfc}\left(\frac{x}{2\sqrt{K\tau}} - \sqrt{\alpha\tau}\right) + e^{\sqrt{\frac{\alpha}{K}}x}\mathrm{erfc}\left(\frac{x}{2\sqrt{K\tau}} + \sqrt{\alpha\tau}\right)\right\}d\tau, \tag{A19}$$

where τ is the integral variable, and the constant α is defined as

$$\alpha = \left(\frac{V}{2\sqrt{K}}\right)^2 + \lambda. \tag{A20}$$

The analytical solution to Eq. (A12), subject to Eqs. (42), (43), and (52), can be obtained using the separation

of variables as given by

$$\bar{c}(x,t) = 1 - \frac{r_2 e^{r_2 L} e^{r_1 x} - r_1 e^{r_1 L} e^{r_2 x}}{r_2 e^{r_2 L} - r_1 e^{r_1 L}} + \sum_{n=1}^{\infty} c_n e^{-(\frac{V}{2K})x} \sin(\sqrt{\mu_n} x) e^{-(\alpha+\mu_n K)t}, \quad \text{(A21)}$$

where r_1 and r_2 are the real distinct roots of the characteristic polynomial equation $Kr^2 - Vr - \lambda = 0$, which can be obtained with

$$r_1, r_2 = \frac{V}{2K} \pm \sqrt{\frac{\alpha}{K}}, \quad \text{(A22)}$$

and μ_n are the roots of the transcendental equation

$$\left(\frac{V}{2K}\right) \tan\sqrt{\mu_n} + \sqrt{\mu_n} = 0, \quad n = 1, 2, 3, \ldots, \infty, \quad \text{(A23)}$$

and c_n is expressed by

$$c_n = \frac{4\sqrt{\mu_n}}{[2L\sqrt{\mu_n} - \sin(2\sqrt{\mu_n} L)]} \times \int_0^L \left(\frac{r_2 e^{r_2 L} e^{r_1 x} - r_1 e^{r_1 L} e^{r_2 x}}{r_2 e^{r_2 L} - r_1 e^{r_1 L}} - 1\right) \times e^{-(\frac{V}{2K})x} \sin(\sqrt{\mu_n} x) dx. \quad \text{(A24)}$$

The steady-state form of Eq. (A12) turns to

$$K\frac{d^2\bar{c}}{dx^2} - V\frac{d\bar{c}}{dx} - \lambda\bar{c} = -\omega. \quad \text{(A25)}$$

Equation (A25) is an inhomogeneous second-order linear ordinary differential equation, which can lead to the following expression for $\bar{c}$ if it is subjected to Eqs. (43) and (52) to find the two integration constants:

$$\bar{c}(x) = 1 - \frac{r_2 e^{r_2 L} e^{r_1 x} - r_1 e^{r_1 L} e^{r_2 x}}{r_2 e^{r_2 L} - r_1 e^{r_1 L}}. \quad \text{(A26)}$$

The local Sherwood number, Sh_x, is defined as the ratio of the gas solute mass flux to the pure diffusive flux at the interface:

$$\mathrm{Sh}_x = -\frac{1}{1-\bar{c}}\frac{\partial c(x, z=0, t)}{\partial z} = -\frac{1}{1-\bar{c}}\frac{\partial c'(x, z=0, t)}{\partial z}. \quad \text{(A27)}$$

A combination of Eqs. (A10), (A26), and (A27) results in

$$\mathrm{Sh}_x = 3 + \frac{7}{40} r_1 r_2 \mathrm{Pe}\left(\frac{e^{r_1 L} e^{r_2 x} - e^{r_2 L} e^{r_1 x}}{r_2 e^{r_2 L} e^{r_1 x} - r_1 e^{r_1 L} e^{r_2 x}}\right). \quad \text{(A28)}$$

The overall Sherwood number can be obtained by averaging Sh_x, Eq. (A28), along the interface:

$$\mathrm{Sh} = \frac{1}{L}\int_0^L \mathrm{Sh}_x dx. \quad \text{(A29)}$$

The integral in Eq. (A29) has been evaluated numerically.

[1] M. Zanfir, A. Gavriilidis, C. Wille, and V. Hessel, Carbon dioxide absorption in a falling film microstructured reactor: Experiments and modeling, Ind. Eng. Chem. Res. **44**, 1742 (2005).

[2] S. A. Gheni, M. F. Abed, E. K. Halabia, and S. R. Ahmed, Investigation of carbon dioxide (CO_2) capture in a falling film contactor by computer simulation, Oil Gas Sci. Technol. **73**, 43 (2018).

[3] R. Custelcean, N. J. Williams, K. A. Garrabrant, P. Agullo, F. M. Brethomé, H. J. Martin, and M. K. Kidder, Direct air capture of CO_2 with aqueous amino acids and solid bis-iminoguanidines (BIGs), Ind. Eng. Chem. Res. **58**, 23338 (2019).

[4] Z. Xu, T. Wang, J. Wu, L. Wang, X. Zhang, H. Dong, and C. Sun, Mass transfer characteristics of CO_2 and blended aqueous solutions of [C_2OHmim][Lys]/MDEA in a microchannel, Ind. Eng. Chem. Res. **62**, 8926 (2023).

[5] M. Khan, D. Nath, M. Khalifi, and H. Hassanzadeh, Measurements and modeling of the dissolution and exsolution kinetics of the ethane/n-heptane system, Ind. Eng. Chem. Res. **62**, 775 (2023).

[6] C. Song, Y. Qiu, M. Xie, J. Liu, Q. Liu, S. Li, L. Sun, K. Wang, and Y. Kansha, Novel regeneration and utilization concept using rich chemical absorption solvent as a carbon source for microalgae biomass production, Ind. Eng. Chem. Res. **58**, 11720 (2019).

[7] M. Danish, R. K. Sharma, and S. Ali, Gas absorption with first order chemical reaction in a laminar falling film over a reacting solid wall, Appl. Math. Model. **32**, 901 (2008).

[8] D. R. Oliver and T. E. Atherinos, Mass transfer to liquid films on an inclined plane, Chem. Eng. Sci. **23**, 525 (1968).

[9] N. Steinfeldt and N. Kockmann, Experimental and numerical characterization of transport phenomena in a falling film microreactor with gas-liquid reaction, Ind. Eng. Chem. Res. **59**, 4033 (2020).

[10] D. Lokhat, A. K. Domah, K. Padayachee, A. Baboolal, and D. Ramjugernath, Gas-liquid mass transfer in a falling film microreactor: Effect of reactor orientation on liquid-side mass transfer coefficient, Chem. Eng. Sci. **155**, 38 (2016).

[11] H. Chinju, K. Uchiyama, and Y. H. Mori, "String-of-beads" flow of liquids on vertical wires for gas absorption, Am. Inst. Chem. Eng. J. **46**, 937 (2000).

[12] Z. Zeng, A. Sadeghpour, G. R. Warrier, and Y. S. Ju, Experimental study of heat transfer between thin liquid films flowing down a vertical string in the Rayleigh-plateau instability regime and a counterflowing gas stream, Int. J. Heat Mass Transf. **108**, 830 (2017).

[13] A. Sadeghpour, Z. Zeng, H. Ji, N. D. Ebrahimi, A. L. Bertozzi, and Y. S. Ju, Water vapor capturing using an array of traveling liquid beads for desalination and water treatment, Sci. Adv. **5**, eaav7662 (2019).

[14] A. Cazaubiel and A. Carlson, Influence of wind on a viscous liquid film flowing down a thread, Phys. Rev. Fluids **8**, 054002 (2023).

[15] A. M. Dashliborun, F. Larachi, and S. M. Taghavi, Gas-liquid mass-transfer behavior of packed-bed scrubbers for floating/offshore CO_2 capture, Chem. Eng. J. **377**, 119236 (2019).

[16] F. Denner, A. Charogiannis, M. Pradas, C. N. Markides, B. G. Van Wachem, and S. Kalliadasis, Solitary waves on falling liquid films in the inertia-dominated regime, J. Fluid Mech. **837**, 491 (2018).
[17] M. A. Zarraa, Y. A. El-Tawil, H. A. Farag, M. Z. El-Abd, and G. H. Sedahmed, Effect of gas sparging on the rate of mass transfer at a single sphere, The Chem. Eng. J. **47**, 187 (1991).
[18] F. H. Shair, Dispersion in laminar flowing liquid films involving heat transfer and interfacial shear, Am. Inst. Chem. Eng. J. **17**, 920 (1971).
[19] O. A. Asbjørnsen, Taylor diffusion in falling liquid films, Chem. Eng. Sci. **28**, 1699 (1973).
[20] S. N. Shah and K. E. Cox, Dispersion in a laminar falling film of an Eyring model fluid, The Chem. Eng. J. **14**, 65 (1977).
[21] G. Taylor, Dispersion of soluble matter in solvent flowing slowly through a tube, Proc. R. Soc. London Ser. A **219**, 186 (1953).
[22] R. Aris, On the dispersion of a solute in a fluid flow through a tube, Proc. R. Soc. London Ser. A **235**, 67 (1956).
[23] B. Berkowitz and J. Zhou, Reactive solute transport in a single fracture, Water Resour. Res. **32**, 901 (1996).
[24] M. Dejam, Advective-diffusive-reactive solute transport due to non-Newtonian fluid flows in a fracture surrounded by a tight porous medium, Int. J. Heat Mass Transf. **128**, 1307 (2019).
[25] M. Dejam, Derivation of dispersion coefficient in an electro-osmotic flow of a viscoelastic fluid through a porous-walled microchannel, Chem. Eng. Sci. **204**, 298 (2019).
[26] Z. Wu and G. Q. Chen, Dispersion in a two-zone packed tube: An extended Taylor's analysis, Int. J. Eng. Sci. **50**, 113 (2012).
[27] R. Datta and V. R. Kotamarthi, Electrokinetic dispersion in capillary electrophoresis, Am. Inst. Chem. Eng. J. **36**, 916 (1990).
[28] T. Y. Lin and E. S. Shaqfeh, Taylor dispersion in the presence of cross flow and interfacial mass transfer, Phys. Rev. Fluids **4**, 034501 (2019).
[29] A. M. Berezhkovskii and A. T. Skvortsov, Aris-Taylor dispersion with drift and diffusion of particles on the tube wall, J. Chem. Phys. **139**, 084101 (2013).
[30] C. O. Ng and Q. Zhou, Dispersion due to electroosmotic flow in a circular microchannel with slowly varying wall potential and hydrodynamic slippage, Phys. Fluids **24**, 112002 (2012).
[31] N. M. Brown and M. Dejam, Tracer dispersion due to non-Newtonian fluid flows in hydraulic fractures with different geometries and porous walls, J. Hydrol. **622**, 129644 (2023).
[32] S. Ghosal, The effect of wall interactions in capillary-zone electrophoresis, J. Fluid Mech. **491**, 285 (2003).
[33] D. R. Webster, D. S. Felton, and J. Luo, Effective macroscopic transport parameters between parallel plates with constant concentration boundaries, Adv. Water Resour. **30**, 1993 (2007).
[34] I. M. Griffiths, P. D. Howell, and R. J. Shipley, Control and optimization of solute transport in a thin porous tube, Phys. Fluids **25**, 033101 (2013).
[35] B. Ling, A. M. Tartakovsky, and I. Battiato, Dispersion controlled by permeable surfaces: Surface properties and scaling, J. Fluid Mech. **801**, 13 (2016).
[36] M. Dejam, H. Hassanzadeh, and Z. Chen, Shear dispersion in a rough-walled fracture, Soc. Pet. Eng. J. **23**, 1669 (2018).
[37] R. Aris, On the dispersion of a solute by diffusion, convection and exchange between phases, Proc. R. Soc. London Ser. A **252**, 538 (1959).
[38] M. Dejam and H. Hassanzadeh, Dispersion tensor in a two-phase flow in a slit, Phys. Fluids **33**, 103612 (2021).
[39] B. Ling, C. B. Rizzo, I. Battiato, and F. P. J. de Barros, Macroscale transport in channel-matrix systems via integral transforms, Phys. Rev. Fluids **6**, 044501 (2021).
[40] M. Dejam and H. Hassanzadeh, Dispersion tensor in stratified porous media, Phys. Rev. E **105**, 065115 (2022).
[41] R. B. Bird, W. E. Stewart, and E. N. Lightfoot, *Transport Phenomena* (Wiley, New York, 1960).
[42] H. B. Fischer, E. J. List, R. C. Y. Koh, J. Imberger, and N. H. Brooks, *Mixing in Inland and Coastal Waters* (Academic Press, San Diego, 1979).
[43] R. N. Horne and F. Rodriguez, Dispersion in tracer flow in fractured geothermal systems, Geophys. Res. Lett. **10**, 289 (1983).
[44] M. N. Özisik, *Heat Conduction* (Wiley, New York, 1993).